# Magnetic field response of NaCl:Eu crystal plasticity due to spin-dependent $Eu^{2+}$ aggregation

R. B. Morgunov and A. L. Buchachenko
*Institute of Problems of Chemical Physics, Chernogolovka 142432, Russia*
(Received 15 December 2009; revised manuscript received 11 July 2010; published 29 July 2010)

Magnetic field impulse (7 T amplitude 10 ms duration) was found to affect microhardness of NaCl:Eu crystals at room temperature. Dimers (pairs of $Eu^{2+}$ paramagnetic ions) were shown to be responsible for the crystal softening induced by magnetic field. Theoretical treatment of the magnetoplastic effect based on the spin dependence of processes resulting in transformation of the dimers in crystals is developed and applied to the description of the long-term magnetic memory. Activation energies of the dimer formation, $E_1 = 0.23 \pm 0.04$ eV and decomposition, $E_2 = 0.33 \pm 0.06$ eV were extracted from thermoactivation analysis of magnetic field controlled $Eu^{2+}$ aggregation in 77–473 K temperature range.

DOI: 10.1103/PhysRevB.82.014115 PACS number(s): 61.72.Cc, 61.72.Hh, 61.72.J−, 61.72.Yx

## I. INTRODUCTION

The effect of magnetic field on dislocation-controlled plasticity of diamagnetic crystals is the phenomenon reliably established and denoted as magnetoplasticity.[1–11] Magnetoplasticity observed in magnetic fields of ~0.1–15 T demonstrates changes in characteristics of plasticity by ~10–100 % at room temperature. Uniqueness of magnetoplastic effects consists in that the energy of interaction of a diamagnetic crystal with magnetic field is negligibly small and, hence, its contribution to high-energy processes of dislocation displacement may also be ignored. Obviously, magnetoplasticity of diamagnetic crystals cannot be interpreted in terms of the energy balance of a stable system since it relates to nonequilibrium intermediate stages of defect interaction. Numerous experiments[1–7] showed that magnetoplasticity originates from the effect of magnetic field on spin-selective generation of paramagnetic states of the short-living "obstacle-dislocation" system.

In ionic crystals, electron transfer between the diamagnetic obstacle ($Ca^{2+}$, $Mg^{2+}$, etc.) and dislocation ($Cl^-$ anion in NaCl as an ionic component of dislocation core) results in generation of spin pairs (for example, $Ca^+$ and Cl).[12,13] Population of the singlet and triplet states of these pairs and the rate of singlet-triplet spin conversion are controlled by Zeeman interaction.[12,13] Coulomb interaction in the spin pairs provides the dislocation capture by obstacles. This interaction is switched off by electron transfer from an obstacle ion to dislocation and controlled by spin orientation in the magnetic field. As a result, the dislocation releases from the obstacle. The singlet spin state lifetime of the $Ca^+$-Cl pair is very short due to fast restoration of the initial electron state of the dislocation captured by the obstacle. Magnetic field stimulates singlet-triplet conversion and populates triplet state which fails to regenerate the initial state of the pair because of forbidden transition from triplet to singlet state. It provides a mechanism stimulating depinning of dislocations and enhancement of their mobility by magnetic field. A similar mechanism is suggested for the magnetoplasticity of both ionic and covalent crystals (germanium, silicon, etc.).[14,15]

The theory of magnetoplasticity developed in Refs. 2 and 12–15 successfully interprets experimental data related to the effect of magnetic field on dislocation path during plastic deformation of diamagnetic crystals. It quantitatively describes "in-field" dislocation mobility enhanced by magnetic field. However, it fails to explain the "out-of-field" magnetoplasticity, i.e., under the conditions when diamagnetic crystals are subjected to magnetic field before deformation and then deformed in the absence of magnetic field. The crystals in this case exhibit so-called "magnetic memory," detected in individual dislocation displacements,[1–7] microhardness,[16–18] macroplastic deformation rate,[19,20] impurity photoluminescence,[21–23] electron spin resonance (ESR) spectra, and magnetization.[11] This kind of magnetic memory has no relation to magnetization of macroscopic ferromagnetic inclusions or nanoparticles. The goal of this paper is to approach theoretically and experimentally the effect of magnetic memory originating from spin-dependent behavior of clusters of paramagnetic ions in diamagnetic crystals.

Association of paramagnetic ions (ion-vacancy dipoles) in dimers (pairs of dipoles) and further aggregation into larger clusters (trimers, tetramers, etc.) are spin-dependent processes which accelerate relaxation of nonequilibrium clusters in magnetic field. Microhardness controlled by dislocation mobility is considered as a response to the restructuring of the dislocation obstacles, induced by magnetic field. We will illustrate the main idea of magnetic memory both theoretically and experimentally for the simplest dimer associates in diamagnetic NaCl crystals doped with paramagnetic $Eu^{2+}$ ions.

## II. THEORETICAL MODELS

First of all, we will demonstrate spin selectivity and magnetic field sensitivity of dimerization of a pair of individual paramagnetic ions. A model ion pair with both ion spins $S = \frac{1}{2}$ will be considered for simplicity. In a contact pair, the binding energy and exchange interaction of ions are high enough to keep the pair in the singlet spin state. Thermal fluctuations activate contact pairs stimulating jumps of the doping ion from the nearest-neighbor position to the next-neighbor lattice site unoccupied by lattice ion (vacancy associated with a doubly charged ion). The state of the pair with distant ions will conventionally be called a separated pair. It inherits total spin of the contact pair and, hence, its initial spin state is also singlet.

 

A spin-selective nanoreactor is a separated pair able to regenerate contact pair by regaining the nearest-neighbor position in a singlet state only. In a triplet state, this process is spin forbidden and the separated pair is supposed to dissociate due to ion diffusion. A competition between the regeneration of the contact pairs and dissociation of the separated pairs is controlled by singlet-triplet spin conversion.

Magnetic field governs triplet-singlet conversion and controls the ratio of separate ions (dipoles) and dimers, and decreases the fraction of the dimers, i.e., magnetic field partly prevents aggregation of dislocation obstacles increasing the concentration of free ions and producing a new nonequilibrium distribution of ions (dipoles) and dimers. In the absence of magnetic field, this phenomenon manifests itself as magnetic memory because of different efficiencies of ion and dimer as dislocation obstacles. Kinetic parameters of the described spin-selective process are shown in Scheme 1 for the model pair of $Cu^{2+}$ ions.

**Scheme 1**

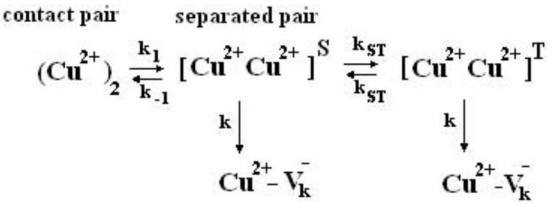


In Scheme 1, reversible conversion of the separated ion pair between singlet and triplet spin states is described by a phenomenological rate constant $k_{ST}$ and decay constant of the ion pair $k$. To express this constant in terms of magnetic field and magnetic parameters of the pair, it is necessary to consider spin dynamics of the pair. Spin functions of the four spin states (singlet S and triplets $T_0, T_+, T_-$ with spin projections $0, 1, -1$) are

$$S = 1/\sqrt{2}(\alpha\beta - \beta\alpha) \quad T_+ = \alpha\alpha,$$

$$T_0 = 1/\sqrt{2}(\alpha\beta + \beta\alpha) \quad T_- = \beta\beta,$$

where $\alpha$ and $\beta$ denote spin states of unpaired electrons of individual ions. In the simplest case, one can neglect exchange interaction and take into account only degenerate states S and $T_0$ keeping in mind that magnetic field cannot mix $T_+$ and $T_-$ states with S and $T_0$. Thus, the time-dependent spin function of the pair may be written as a linear combination of S and $T_0$ states,

$$\varphi(t) = C_S(t)S + C_{T0}(t)T_0. \tag{2.1}$$

Coefficients $|C_S(t)|^2$ and $|C_{T0}(t)|^2$ are the probabilities for the pair to be in the singlet or triplet states, respectively. To determine these coefficients it is necessary to solve the time-dependent Schrödinger equation,

$$i\,\partial\varphi/\partial t = \hat{H}\varphi \tag{2.2}$$

with Hamiltonian,

$$\hat{H} = \beta H(g_1 S_1 + g_2 S_2), \tag{2.3}$$

where $S_1$ and $S_2$ are spins of partners, $g_1$ and $g_2$ are their $g$ factors, $H$ is magnetic field. Substituting Eqs. (2.1) and (2.3) to the Eq. (2.2) and calculating matrix elements $\langle S|\hat{H}|S\rangle$, $\langle T_0|\hat{H}|T_0\rangle$, and $\langle S|\hat{H}|T_0\rangle$ one can derive

$$|C_S(t)|^2 = \sin^2(1/2\Delta g\beta H)t. \tag{2.4}$$

This coefficient characterizes the rate of triplet-singlet spin conversion assuming the initial state to be triplet, i.e., $|C_S(t)|^2=0$. The same expression is valid for the singlet pair to be transformed to its triplet state. Equation (2.4) describes oscillating time-dependent spin evolution of the pair. Evolution time is restricted by the lifetime $\tau$ of the pair.

To determine the probability for the initially singlet pair to transform to the triplet state, a function $f(t)$ is introduced, which characterizes time-dependent probability for the separated pair to decay,

$$f(t) = 1/\tau \exp(-t/\tau), \tag{2.5}$$

where $\tau$ is the lifetime of the pair, $\tau=(2k)^{-1}$, and $f(t)$ is normalized according to $\int f(t)dt=1$. Then probability $P$ of a singlet pair to convert into the triplet one is

$$P = \int f(t)|C_S(t)|^2 dt. \tag{2.6}$$

Substituting Eqs. (2.4) and (2.5) into Eq. (2.6), one obtains

$$P = (\Delta g\beta H/4k)^2/[1 + (\Delta g\beta H/2k)^2]. \tag{2.7}$$

It can be seen that the magnetic field induced spin evolution of the pair is a function of the ratio $\Delta g\beta H/2k$ which characterizes competition between spin and chemical dynamics. Designating $(\Delta g\beta H/k)$ as $\varphi$ the Eq. (2.7) may be reduced to

$$P = (\varphi/4)^2/[1 + (\varphi/2)^2]. \tag{2.8}$$

The limiting value of $P$ at $\varphi\to\infty$ is $\frac{1}{4}$; it follows from the fact that we considered only one channel of spin conversion, S-$T_0$, and ignored the two others.

Three important features should be noted. First, we considered the simplest spin nanoreactor of two ions with spins $S=\frac{1}{2}$. For $Eu^{2+}$ ion $S=7/2$ a total number of spin states equal to $2S+1=15$. Among them, only one state with $S=0$ can regenerate the singlet state of the contact pair. All other high-spin (HS) states dissociate into separated individual ions. However, during the lifetime of the nanoreactor ($\sim 10^{-8}-10^{-6}$ s) magnetic field stimulates transitions from singlet to high-spin states and lowers the probability of regeneration of the initial contact pair. Virtually, the fraction of single ions increases in magnetic field and the fraction of dimers decreases.

Second, spin conversion in the nanoreactor is induced by magnetic interactions. However, the question of which interactions are responsible for spin conversion is still open. In a separated pair of chemically identical ions (for example, $Cu^{2+}$ or $Eu^{2+}$), their $g$ factors are considered to be equal. However, it is well known from ESR spectroscopy that $g$

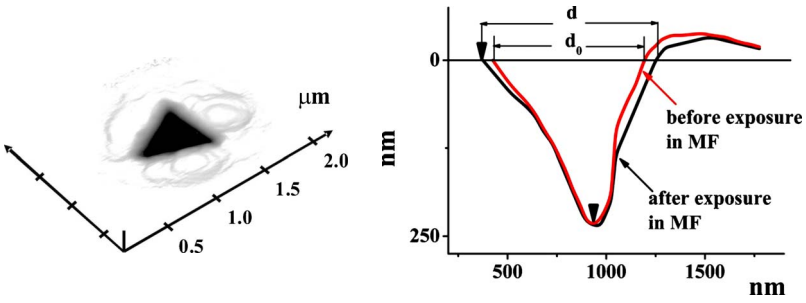


FIG. 1. (Color online) (a) Indentation imprint and (b) its profile obtained by scanning of crystal surface with AFM.

factors of ions located in different lattice sites can slightly differ ($\Delta g \sim 10^{-3}$). This small difference in $\Delta g$ results in the difference of Zeeman energies $\Delta g \beta H$ which induces spin conversion. For chemically different ions, such as $Fe^{3+}$ and $Fe^{2+}$, $Eu^{2+}$ and $Co^{3+}$, etc., their $g$ factors can strongly differ. Thus, spin conversion in asymmetric pairs is faster and accumulated magnetic memory can be significant.

Moreover, spin conversion can proceed via relaxation mechanism. Then the field dependence of longitudinal and transverse relaxation times $T_1$ and $T_2$ can provide magnetic field effect. Though neither $T_1$ nor $T_2$ can separately induce S-T transitions, their cooperative effect results in stochastic relaxation and spin conversion.

Third, three processes compete in a spin nanoreactor, namely, regeneration of a contact pair (in a singlet state), nanoreactor decomposition into individual ions, and spin conversion. Characteristic time of the processes is $10^{-8}-10^{-6}$ s. These processes provide a new distribution of ions and clusters in magnetic field. In principle, one can imagine two extreme situations concerning magnetic memory. If paramagnetic ions are homogeneously distributed in crystals in the beginning, magnetic field accelerates their association since it stimulates spin conversion of triplet states of encounter ion pairs (their fraction being $\frac{3}{4}$ of the total encounters) into the singlet state. Oppositely, if ions are initially present as dimers, magnetic field will accelerate disintegration of dimers into the monomer ions. In both cases, memory effects are expected to be observable. However, time evolution of the effects is different depending on the initial distribution of paramagnetic ions.

## III. EXPERIMENT

Crystal plasticity was characterized by microhardness $Mh$, which was measured as follows. First, microindentation of the sample surface (001) was performed using constant load applied to a trilateral pyramid (Berckovich indentor) with tip radius about 25 nm. Loading was performed using a microhardness meter of a Neophot optical microscope. The 20–30 microhardness indentation imprints were created on the surface and then used in calculations of errors and average values. Indentation imprint size $\boldsymbol{d}$ was determined using an Integra NT-MDT atomic force microscope. Figure 1 shows the indentation imprint profile obtained by atomic force microscopy (AFM) scanning. Gage elasticity constant value was 290 N/m, resonance frequency was 75 kHz, and load was 400 $\mu$N. Sapphire single crystal with Young's modulus $E=470$ GPa was used as an ⟨⟨ideally hard⟩⟩ reference sample.

Microhardness $Mh$ was calculated using standard Berckovich formula: $Mh=2092P/\boldsymbol{d}^2$, where $P$ is a load and $\boldsymbol{d}$ is an indentation size. It was found from the observation of indentation imprints by optical microscope that the edge contrast is enough to provide 1% relative accuracy of $Mh$ measurement. The absolute value of the microhardness was calibrated using the AFM data. In aged nontreated (thermally or magnetically) samples, absolute value of microhardness was $Mh=152\pm2$ MPa independently of the point on the homogeneous crystal surface.

Magnetic field impulse was generated in a low-resistance solenoid by 800 A electric pulse. The field impulse had sinusoidal shape with half-period duration of 10 ms, 7 T amplitude. It is seen from Fig. 1(a) that the indentation imprint has larger size due to the effect of magnetic field pulse on quenched crystals stored after quenching at room temperature for $t_{\text{pause}}=45$ h (the reason for this time delay will be explained below). The difference $\Delta Mh=Mh_2-Mh_1$ between microhardness measured after and before application of the magnetic field impulse was used as a quantitative characteristics of the magnetoplasticity. Measurements of $\Delta Mh$ were performed during 10 min, which is much shorter than the aggregation time under current experimental conditions. Thermal treatment itself affects the absolute value of microhardness $Mh$. However, this effect was not studied in our work. As shown below, maximal observed magnetic field effect $\Delta Mh=20$ MPa corresponds to the relative change in microhardness, $\Delta Mh/Mh=13\%\pm1\%$.

The crystals were annealed at 770 K in Ar atmosphere and then quickly cooled down to room temperature on a large copper plate. The pause between quenching and microhardness measurements provides time for the formation of the simplest clusters (dimers) by diffusion. Without such pause, microhardness was not affected by magnetic field. The sequence of the procedures is shown in Fig. 2(a). Temperature and duration of the first annealing $t_{\text{annealing1}}$, pause between quenching $t_{\text{pause}}$, temperature, at which the sample was stored during this pause $T_{\text{pause}}$, as well as the temperature of the second annealing $T_{\text{annealing2}}$, were varied in the experiments. Conditions for indentation and application of the magnetic field impulse were similar in all experiments.

Special attention was paid to avoid the artifacts during microhardness measurements. Reference samples stored in conditions similar to those for magnetically treated ones were indented and tested to make sure that humidity, small temperature variations and other nonmagnetic factors did not affect the microhardness.

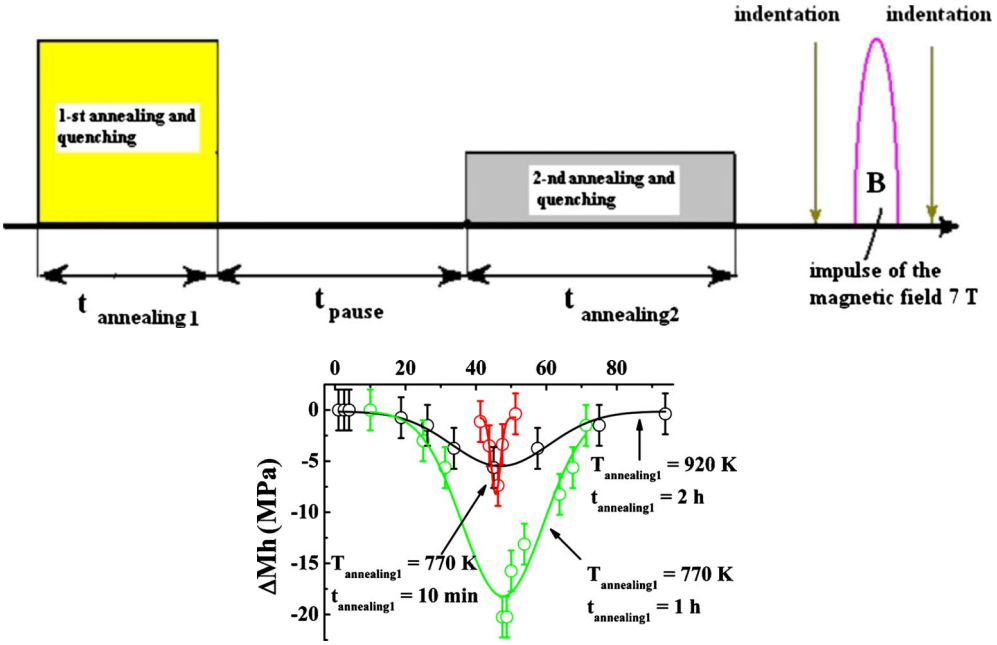


FIG. 2. (Color online) (a) Time sequence of thermal quenching procedure, microhardness measurement, and magnetic field pulse application. (b) Microhardness change $\Delta Mh$ caused by magnetic field (MF) pulse as a function of time interval $t_{pause}$ after the first quenching (1 h storage at $T_{annealing1}=770$ K and cooling to 293 K). Three different regimes of annealing temperature $T_{annealing1}$ and quenching duration $t_{annealing1}$ are shown.

## IV. RESULTS AND DISCUSSION

Strategy of our experiments is based on well-known facts related to $Eu^{2+}$ ion properties in NaCl crystal lattice:[24–26] (1) $Eu^{2+}$ ion is coupled with vacancy $V_{Cl^-}$ and present as impurity-vacancy dipole to compensate extra charge in the NaCl lattice. An individual $Eu^{2+}$ ion has high free energy and negligibly small concentration. Thus, $Eu^{2+}$ dipoles are simplest building blocks for cluster formation. (2) Heating of the aged crystals above $T=500$ K (annealing) leads to dissolution of the $EuCl_2$ precipitates and their conversion into separated individual impurity-vacancy dipoles. Activation energies of the cluster decomposition are high enough to prevent the disintegration of the clusters below 500 K. (3) The dissolved state of $Eu^{2+}$ dipoles can be stabilized by fast cooling of the crystals down to room temperature (quenching). At room temperature, diffusion mobility of the dipoles is suppressed, resulting in aggregation dynamics slow enough for our experiments. (4) Heating of the crystals in the range $300<T<500$ K accelerates the $Eu^{2+}$ dipoles diffusion with no effect on the clusters decomposition.

Taking into account these facts, we used the following sequence of experimental operations sketched in Fig. 2(a): (1) thermal decomposition of the $EuCl_2$ precipitates by first annealing was accompanied by first quenching down to room temperature. In the majority of experiments, $T_{annealing1}$ was 770 K. Only in the first series of experiments, $T_{annealing1}$ was varied in 770–920 K range and annealing duration was 10–120 min to verify whether annealing time was sufficient for dissolution of all precipitates. (2) Pause $t_{pause}$ was varied to probe slow diffusion of the $Eu^{2+}$ dipoles and its aggregation into small clusters at room temperature. As is shown below, there is no magnetoplasticity in the crystals containing fully dissolved $Eu^{2+}$ dipoles. For this reason, the pause is necessary for aggregation of the dipoles into clusters providing magnetoplasticity. (3) Second annealing at lower temperature ($T_{annealing2}$ below 500 K) was followed by second quenching down to 300 K. Second annealing was used to accelerate $Eu^{2+}$ dipole diffusion and to obtain small clusters faster than at room temperature. Low-temperature annealing does not decompose the precipitates, keeping constant dipole concentration.

The procedures of thermal treatment allowed us to prepare different kinds of crystals, mainly those containing dispersed dipoles or small clusters of the dipoles (dimers, trimers, etc.), or large clusters and precipitates, or combinations of all these defects. This enabled studies of the effect of $Eu^{2+}$ clusterization and cluster dissolution on magnetoplastic effect. After the thermal treatment, measurements of the microhardness response on the application of the magnetic field impulse were performed. The final result of our experiments was the $\Delta Mh$ value as a function of thermal treatment parameters. The experiments described allowed us to determine the types of the $Eu^{2+}$ defects responsible for the magnetoplastic effect.

### A. Effect of precipitates dissolution on the magnetoplasticity

Since the efficiency of cluster decomposition depends on temperature and annealing period, in the first series of experiments we studied the effect of cluster dissolution on the magnetoplasticity value $\Delta Mh$. Therefore, annealing time before quenching and annealing temperature were varied. Dissolution of precipitates is the source of the precursors X (mainly dipoles) necessary for the subsequent formation of the magnetosensitive clusters.

Figure 2(b) shows the dependence of the magnetoplastic effect $\Delta Mh$ on time pause $t_{pause}$ after quenching. Three quenching conditions were studied: (1) the crystals were stored at $T=920$ K for $t_{annealing1}=2$ h; (2) the crystals were stored at $T_{annealing1}=770$ K for $t_{annealing1}=1$ h; (3) the crystals were stored at $T_{annealing1}=770$ K for $t_{annealing1}=10$ min. Then all crystals were rapidly cooled down to room temperature. The second annealing was not used ($t_{annealing2}=0$) in this series. Figure 2(b) shows the maximum of the magnetoplastic effect at $t_{pause}=45$ h, which was independent of the first annealing conditions in contrast to the maximal value of the magnetoplastic effect $\Delta Mh_{max}$ sensitive to the thermal pretreatment. These data allowed making the following conclusions: (1) magnetic field does not affect dipoles arising in the crystals immediately after annealing and quenching at $t_{pause}=0$. (2) Observation of the magnetoplasticity requires products aggregation, which maximal amount corresponding to maximal magnetoplasticity $\Delta Mh_{max}$ at $t_{pause}=45-50$ h. (3) Kinetics of the precursor aggregation at 300 K is independent of the thermal prehistory that controls the amount of aggregation products and the maximal value of magnetoplastic effect.

At $T_{annealing1}=770$ K, the diffusion coefficient of the $Eu^{2+}$ ions, $D\sim 10^{-20}$ $m^2$ $s^{-1}$; the diffusion path for $t_{pause}=6\times 10^2$ s is $L_1\sim(6Dt_{pause})^{1/2}\sim 6\times 10^{-9}$ m. Taking into account the diffusion activation energy of $E\sim 0.7$ eV,[27] one can assume that average distance $L_2$ is almost 30 times longer than $L_1$ corresponding to complete decomposition of the clusters at $T_{annealing1}=920$ K and $t_{annealing1}=2$ h. The ratio of the dipole displacements in these experiments would be $\sim(L_2/L_1)^2\sim 10^3$. Nevertheless, it does not affect the position of the maximum of the magnetoplastic effect on the $\Delta Mh(t_{pause})$ curve. Thus, we can conclude that kinetics of the $Eu^{2+}$ dipole aggregation is not sensitive to the variation in the heat treatment conditions. It provides an opportunity of reliable comparison of aggregation kinetics in the second series of the experiments. The above-discussed estimation shows that the dimers (couples of the dipoles) are responsible for magnetoplasticity since there is no time for diffusion-controlled formation of more complex clusters.

### B. Kinetics of the temperature controlled accumulation of magnetosensitive dipoles

In the second series of experiments, we studied kinetics of the dimer D formation by aggregation of precursors X (dipoles), liberated from the initial clusters by annealing of the crystals. Thus, the X→D process was under study in this series. Intermediate heat treatment conditions, discussed above, i.e., $T_{annealing1}=770$ K, $t_{annealing1}=1$ h were chosen. After this treatment and crystal quenching down to room temperature, the pause $t_{pause}$ was used prior to $\Delta Mh$ measurement. $T_{pause}$ was 77, 393, or 473 K. After the pause, temperature was restored to 293 K, microhardness was measured, and its change caused by magnetic field, $\Delta Mh$, was determined. Figure 3 shows the $\Delta Mh(t_{pause})$ dependencies at three temperatures $T_{pause}=77$, 393, and 473 K. It was found that the increase in $T_{pause}$ shifts the position of the $\Delta Mh(t_{pause})$ maximum to shorter times (Fig. 3), i.e., temperature-controlled aggregation rate modulates magnetoplasticity.

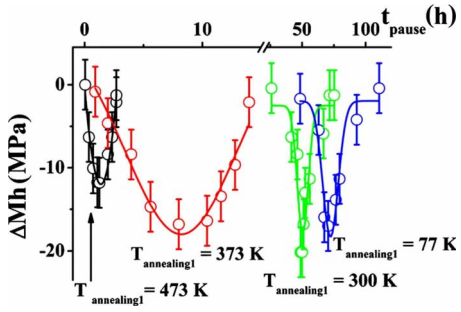


FIG. 3. (Color online) Microhardness change $\Delta Mh$ caused by MF pulse as a function of the time interval $t_{pause}$ passed after crystal quenching from $T_{annealing1}=770$ K when the quenched crystals were kept at $T_{pause1}=77$, 300, 373, and 473 K.

Note that the temperatures $T_{pause}=77$, 393, and 473 K are all below 500 K, i.e., cluster decomposition does not contribute to magnetoplasticity. Kinetics of $\Delta Mh$ is controlled by the $Eu^{2+}$ dipole migration. Thus, heating of the crystals up to $T_{pause}=473$ K during pause leads to acceleration of the dipole aggregation and faster generation of the dimers responsive to applied magnetic field. Larger clusters cannot be formed during the 10–50 h pause because of limitations in the $Eu^{2+}$ dipoles diffusion path $L$. Freezing of the $Eu^{2+}$ aggregation at the lowest temperature $T_{pause}=77$ K delays mobility of dimer precursors (dipoles) and decelerates the formation of dimers responsible for the magnetoplasticity.

According to Refs. 24–26, the temperature increase accelerates not only diffusion rate but also aggregation process. The dimers emerging within the crystal lattice at the beginning of the aggregation can be destroyed by heating. The other possible way of the dimer transformation to the state insensitive to magnetic field is a capture of the next-neighbor dipoles (transformation to a trimer) as well as intradimer transformations described in Ref. 26. Thus, the existence of maximum on the $\Delta Mh(t_{pause})$ dependence should be explained by a competition between the diffusion-controlled generation of magnetoresponsive dimers, which provide magnetoplasticity, and by transformations of these dimers to another product (decomposition of dimers, capture of additional $Eu^{2+}$ dipoles, intradimer rearrangements). It implies that thermal fluctuations provide accumulation of dimers D as well as their decomposition and conversion to aggregation products Y insensitive to magnetic field. Thus, dimers accumulation in the crystal depends on a ratio of the rates of their formation X→D and conversion to subsequent aggregation products D→Y.

### C. Transformation kinetics of the accumulated magnetosensitive dimers

The goal of the third series of experiments was to accumulate the largest amount of the magnetosensitive dimers D during the pause and to observe kinetics of their magnetosensitive transformation to the products Y. Thus, D→Y process was of dominant interest. In this series immediately after attaining the maximal $\Delta Mh_{max}$ value ($t_{pause}$

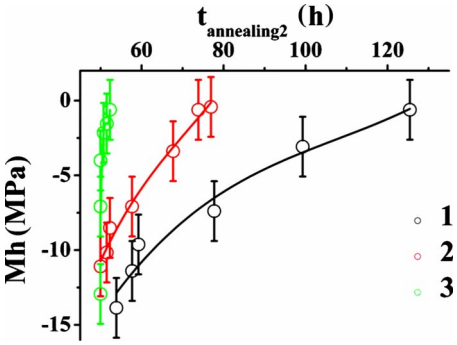


FIG. 4. (Color online) Dependencies of microhardness change $\Delta Mh$ caused by MF pulse on time $t_{\text{annealing2}}$ passed during the second crystal quenching. The crystal was stored after the first quenching ($t_{\text{annealing1}}=1$ h storage at $T_{\text{annealing1}}=770$ K and cooling to 293 K) for $t_{\text{pause}}=50$ h and then temperature was stabilized at (1) $T_{\text{annealing2}}=77$, (2) 293, and (3) 473. Microhardness measurements and magnetic field application were performed at 293 K.

$\sim 45$ h, $T_{\text{pause}}=300$ K), when one could assume the process of dimer accumulation to be less efficient than their decomposition, temperature was changed, and the crystal was kept at lower temperature $T_{\text{annealing2}}$ for the time $t_{\text{annealing2}}$ (Fig. 4). Crystal cooling results in considerable deceleration of spontaneous decrease in the magnetoplastic effect (Fig. 4). The rate of the decrease in the magnetoplastic effect becomes lower at lower temperatures indicating a decrease in D. Since accumulation of the dimers is basically over at $t_{\text{pause}}\sim 45$ h, we can consider Fig. 4 as a time dependence of the magnetoplasticity modulated by kinetics of the subsequent dimer transformations $\text{D}\rightarrow\text{Y}$. Diffusion-controlled aggregation $\text{X}\rightarrow\text{D}$ may be neglected.

### D. Thermoactivation analysis of the subsequent aggregation stages

Change in microhardness $\Delta Mh$ caused by external magnetic field is an indirect response to the processes occurring in a subsystem of the $Eu^{2+}$ defects. Nevertheless, considering the obvious fact that crystal softening under magnetic field $\Delta Mh$ increases with dimer amount D, one can perform thermoactivation analysis assuming proportionality $\Delta Mh(t) \propto \text{D}(t)$ applicable for small variations in the $Mh$ and $N$ values.

Kinetics of dimer concentration after quenching may be described by the following system of consecutive reactions:

$$\rightarrow X \xrightarrow{k_{XD}} D \xrightarrow{k_{DY}} Y \rightarrow \ldots, \quad (4.1)$$

where X is the dipole precursor of the magnetosensitive dimer; D is the magnetosensitive dimer; Y are the products arising after the dimer stage of aggregation (for example, trimers); $k_{\text{XD}}$ and $k_{\text{DY}}$ are the reaction-rate constants, $k_{\text{XD}}=k_{0\text{XD}}\exp(-E_{\text{XD}}/k_{\text{B}}T)$, $k_{\text{DY}}=k_{0\text{DY}}\exp(-E_{\text{DY}}/k_{\text{B}}T)$; $E_{\text{XD}}$ is the activation energy of the preaggregation stages $\text{X}\rightarrow\text{D}$ of the dimer formation, $E_{\text{YD}}$ corresponds to activation energy of the decomposition of the dimer $\text{D}\rightarrow\text{Y}$ and its transformation into Y products.

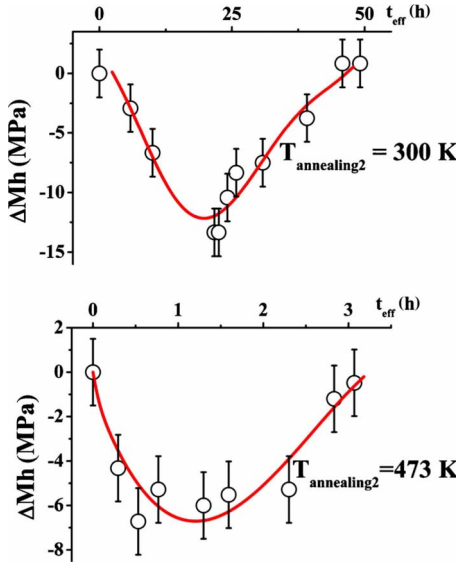


FIG. 5. (Color online) Microhardness change $\Delta Mh$ caused by MF pulse as a function of the time $t_{\text{eff}}$ passed after the first quenching from $T_{\text{annealing1}}=770$ K in conditions when the quenched crystals were stored at (a) $T_{\text{pause}}=300$ K and (b) $T_{\text{pause}}=473$ K. Dots are experimental data; lines are approximations of the experimental data by formula (2.3).

Since the position of the maximum magnetoplasticity effect does not depend on temperature and time of the first annealing (Fig. 2), a conclusion can be drawn that the accumulation of dimers in a crystal can be described by the two reactions: $\text{X}\rightarrow\text{D}\rightarrow\text{Y}$. Since the starting dipole migration stage is unknown, additional delay parameter $t_0=25$ h, determined from the approximation discussed below was introduced. Kinetics of $Mh$ replotted vs $t_{\text{eff}}=t-t_0$ is shown in Figs. 5(a) and 5(b).

For the monomolecular reactions, the equation system for reagent concentrations is

$$\frac{d\text{X}}{dt} = -k_{\text{XD}}\text{X},$$

$$\frac{d\text{D}}{dt} = k_{\text{XD}}\text{X} - k_{\text{DY}}\text{D},$$

$$\frac{d\text{Y}}{dt} = k_{\text{DY}}. \quad (4.2)$$

Dimer concentration is determined from the above equation system as

$$\text{D}(t) = \frac{Nk_{\text{XD}}}{k_{\text{XD}}-k_{\text{DY}}}\{[\exp(-k_{\text{DY}}t) - \exp(-k_{\text{XD}}t)]\}. \quad (4.3)$$

The approximations of the experimental $\Delta Mh(t_{\text{eff}})$ dependence using formula (4.3) are shown in the Fig. 5 for 300 and 473 K.

The values of activation energies and pre-exponential factors for accumulation and disappearance of dimers were determined to be $E_{\text{XD}}=0.23\pm0.04$ eV, $k_{0\text{XD}}=(3.6\pm1.1)$

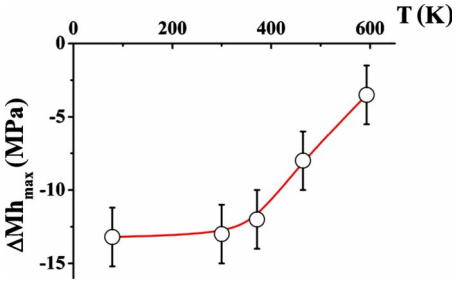


FIG. 6. (Color online) Maximal change in microhardness $\Delta Mh_{\max}$ caused by MF pulse as a function of temperature $T_{\text{pause}}$ at which the crystal was stored after the first quenching from $T_{\text{annealing1}}=770$ K. Dots—experiment, line—approximation of experimental data according to formula (2.4).

$\times 10^5$ $s^{-1}$ and $E_{\text{DY}}=0.33\pm0.06$ eV, $k_{0\text{DY}}=(2.0\pm0.5)\times 10^6$ $s^{-1}$, respectively. The difference of activation energies of the X→D and D→Y reactions is $\Delta E=E_{\text{DY}}-E_{\text{XD}}=0.1$ eV.

The $\Delta E$ value can be determined independently from the data presented in Fig. 6. The difference $\Delta E$ can be derived more precisely by fitting the temperature dependence of magnetoplastic effect in its maximum, $\Delta Mh_{\max}$. The value of maximal concentration of dimers, $D_{\max}$, as derived from formula (4.3) is

$$D_{\max}=Np^{1/1-p}, \tag{4.4}$$

where $p=k_{\text{XD}}/k_{\text{DY}}=(k_{0\text{XD}}/k_{0\text{DY}})\exp[(E_{\text{DY}}-E_{\text{XD}})/k_{\text{B}}T]$.

Since magnetic field affects the dimers, the maximal magnetoplastic effect is observed when the maximum number of magnetosensitive dimers D is present. Formula (4.4) adequately describes the $\Delta Mh_{\max}(T_{\text{pause}})$ dependence (Fig. 6). The difference of activation energies of accumulation and decomposition of magnetosensitive defects extracted from this approximation, $\Delta E=E_{\text{DY}}-E_{\text{XD}}=0.14\pm0.03$ eV, is close to the above estimated $\Delta E=0.1$ eV. Since $\Delta Mh_{\max}(T_{\text{pause}})$ and $\Delta Mh(t_{\text{pause}})$ dependences were approximated independently, similarity of the $\Delta E$ values justifies correctness of the approximation used. Values of the activation energies were compared with energies of different processes in the subsystem of impurity ions independently measured and reported in Refs. 24–26. It was found that the extracted activation energies are close to the bond energy of low-atomic clusters and to the energy of elastic restoration of clusters by $Eu^{2+}$ jumps from exact positions of $Na^+$. Thus, one can suppose that magnetic field causes changes in atomic structure of dimeric $Eu^{2+}$ clusters. As a result of cluster transformation, elastic fields of these clusters change. Cluster elastic field is the main factor controlling cluster interaction with moving dislocation. Thus, the changes in microhardness observed under magnetic field are due to magnetic field effect on the $Eu^{2+}$ dimers.

### E. Spin-dependent kinetics of the dimer D→Y transformation

Kinetics of dimer transformation into isolated ions is considered for the $(Eu^{2+})_2$ dimer dissociating to $Eu^{2+}$ dipoles (electron spin $S=7/2$). This dimer, i.e., a contact pair of ions is assumed to dissociate with the rate constant $k_1$ in such a way that one of the ions moves to a neighboring lattice site generating a separated pair in the singlet spin state (Scheme 2). The separated pair is a spin nanoreactor in which reversible spin conversion between singlet (spin $S=0$) and high-spin ($S=1,2,\ldots,7$) states (HS) occurs with the rate constant $k_{\text{HS}}$. The reverse reaction, i.e., conversion of separated pair into the initial contact pair, is spin allowed for the singlet state (with the rate constant $k_{-1}$) and spin forbidden for the high-spin states. The separated pair further dissociates into individual ions from both states (S and HS) with the rate constant $k$.

Scheme 2

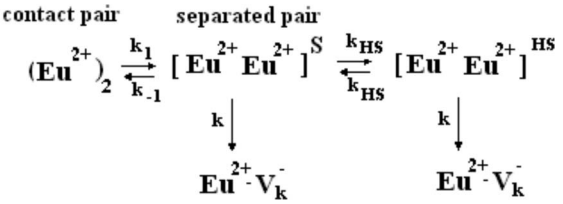


Scheme 2 includes four types of species, namely, dimer D, individual ions $M$ and two states, S and HS, in a spin nanoreactor. Time evolution of their concentrations is described by kinetic equations,

$$-d[\text{D}]/dt=k_1[\text{D}]-k_{-1}[\text{S}], \tag{4.5}$$

$$d[\text{S}]/dt=k_1[\text{D}]+k_{\text{HS}}[\text{HS}]-(k_{-1}+k+k_{\text{HS}})[\text{S}]=0, \tag{4.6}$$

$$d[\text{T}]/dt=k_{\text{HS}}[\text{HS}]-(k+k_{\text{HS}})[\text{HS}], \tag{4.7}$$

$$d[M]/dt=k([\text{S}]+[\text{HS}]). \tag{4.8}$$

Taking into account that concentration of separated pairs may be considered to be quasistationary, the following equations can be derived:

$$[\text{D}]=[\text{D}_0]\exp(-\alpha t), \tag{4.9}$$

$$[M]=[\text{D}_0][1-\exp(-\alpha t)], \tag{4.10}$$

where $[\text{D}_0]$ is the initial concentration of dimers.

Here the values of $\alpha$ are $\alpha_{\text{H}}$ and $\alpha_0$ for the process in magnetic field $H$ and for zero magnetic field, respectively. Then

$$(dM/dt)_0=\alpha_0\exp(-\alpha_0 t), \tag{4.11}$$

$$(dM/dt)_{\text{H}}=\alpha_{\text{H}}\exp(-\alpha_{\text{H}} t), \tag{4.12}$$

where

$$\alpha_{\text{H}}=[k_1k(2k_{\text{HS}}+k)]/[(k_{-1}+k+k_{\text{HS}})(k_{\text{HS}}+k)-k_{\text{HS}}^2], \tag{4.13}$$

$$\alpha_0=k_1k/(k_{-1}+k). \tag{4.14}$$

The latter follows from Eq. (4.13) at $k_{\text{HS}}=0$. Introducing dimensionless factor

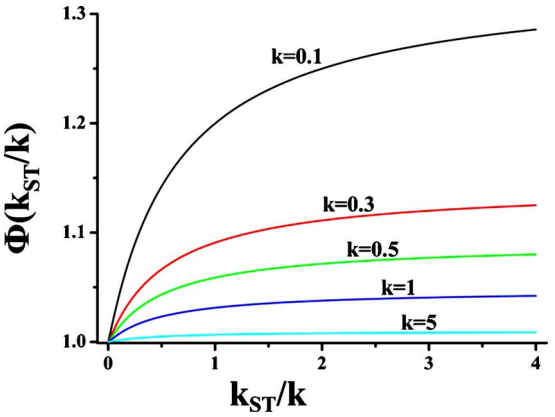


FIG. 7. (Color online) Calculated dependences $\Phi(k_{ST}/k)$ of dimer dissociation rate after magnetic field application on the reaction-rate constant ratio, $k_{ST}/k$, proportional to magnetic field $H$. The dependences are shown for different $k$ values.

$$\varphi = [M]/[D_0], \tag{4.15}$$

one can derive a general equation

$$\Phi = [d\varphi_H/dt]_H/[d\varphi_0/dt]_0 = \alpha_H/\alpha_0 \exp[(\alpha_0 - \alpha_H)t]. \tag{4.16}$$

The $\Phi$ value determines quantitatively magnetic memory as the ratio of dimers dissociation rate (or generation of single ions) in magnetic field $H$ to that in zero magnetic field.

Magnetic memory $\Phi$ is a function of the rate constants $k_1$, $k_{-1}$, and $k$, which are independent of magnetic field $H$, and the rate of spin conversion $k_{HS}$. One can introduce a dimensionless ratio $k_{HS}/k$ and calculate the memory effect $\Phi$ as a function of this ratio. Figure 7 demonstrates the $\Phi(k_{ST}/k)$ dependence for several $k$ values. The $\Phi(H)$ corresponds a field dependence because $k_{ST}/k \sim H$. At $k_{ST}=0$ $(H=0)$, there is no magnetofield effect, i.e., $\Phi(0)=1$ and with increasing $k_{ST}$ it reaches the maximum of approximately 30%. It should be noted that this value is smaller than the maximal magnetoplastic effect observed in our experiments on microhardness $\Delta Mh/Mh$ approximately 13%.

The existence of the limit is due to the reversibility of spin conversion. At fast spin conversion $(k_{ST} \gg k)$ populations of both spin states, S and T, become equal, and initial dissociation rate of dimers $(t=0)$ attains its maximum.

The dependences of field-effect efficiency of the dimer dissociation, $\Phi$, on the field strength $H$ (proportional to $k_{ST}/k$) and dissociation constants $k$ may be presented as a surface (Fig. 8) which allows finding optimal conditions for the magnetoplastic effect. This surface can be used to explain why magnetic memory can be generated by short magnetic field pulse if its strength is high enough.

In general, an inverse problem can be solved if magnetic field effect is calculated in the rate of separated ions recombination and conversion to the dimer. This process is also dependent on $k_{ST}$. The equations describing kinetics of ions association to dimers are more complicated and not presented here. It should be noted that the physical mechanism of magnetic field effect in this process is almost similar to that for the case of dimers dissociation.

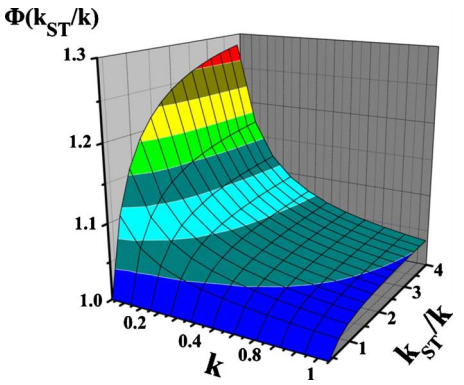


FIG. 8. (Color online) Calculated dependence $\Phi(k_{ST}/k)$ of dimer dissociation rate after magnetic field application on reaction-rate constants ratio, $k_{ST}/k$, proportional to the magnetic field $H$ and dimer decay rate constant, $k$, for $t=0$.

## V. CONCLUSIONS

Magnetic field was shown to affect microhardness of NaCl:Eu crystals. The most intriguing and remarkable feature of magnetoplasticity is that the changes in plasticity of diamagnetic NaCl:Eu crystals can be observed after magnetic field application. Thus, magnetic field induced changes are conserved for a long time in the absence of magnetic field. The suggested mechanism of this phenomenon is named as magnetic memory and is based on the spin dependence of processes resulting in transformation of dimers into separated paramagnetic $Eu^{2+}$ ions. Spin-dependence results in the yield of dimers in magnetic field different from that in zero magnetic field. Since the rates of dislocation depinning from isolated ions (dipoles) and dimers are different, plasticity of crystals subjected to magnetic field is different from that of crystals which were not exposed to magnetic field. The difference in plasticity of crystals with different magnetic prehistory is a quantitative measure of magnetic memory. The latter decays gradually when magnetic field is removed, with the rate controlled by diffusion of paramagnetic ions or dissociation of the dimers.

Magnetic memory as a physical phenomenon can be of technical and technological interest in solid-state physics and material science. It can be controlled by the concentration of different paramagnetic ions, by varying temperature and magnetic field strength as well as by combination of all these factors.

## ACKNOWLEDGMENTS

The authors are grateful to V. I. Al'shits and I. I. Proskuryakov for helpful discussions.

[1] V. I. Alshits, E. V. Darinskaya, M. V. Koldaeva, and E. A. Petrzhik, in *Dislocations in Solids: A Tribute to F.R.N. Nabarro*, edited by J. P. Hirth (Elsevier, Amsterdam, 2008), Vol. 14, p. 333, Chap. 86.

[2] V. I. Alshits, E. V. Darinskaya, M. V. Koldaeva, and E. A. Petrzhik, J. Appl. Phys. **105**, 063520 (2009).

[3] Yu. I. Golovin and R. B. Morgunov, *Chemistry Reviews, Part 2* (Gordon and Breach, New York, 1998), Vol. 23, p. 23.

[4] Yu. I. Golovin, R. B. Morgunov, and A. A. Baskakov, Mol. Phys. **100**, 1291 (2002).

[5] M. V. Badylevich, V. V. Kveder, V. I. Orlov, and Yu. A. Ossipyan, Phys. Status Solidi C **2**, 1869 (2005).

[6] V. A. Makara, L. P. Steblenko, Yu. L. Kolchenko, S. M. Naumenko, O. A. Patran, V. M. Kravchenko, and O. S. Dranenko, Solid State Phenom. **108-109**, 339 (2005).

[7] I. Yonenaga and K. Takahashi, J. Appl. Phys. **101**, 053528 (2007).

[8] M. I. Molotskii and V. Fleurov, Phys. Rev. Lett. **78**, 2779 (1997).

[9] M. Molotskii and V. Fleurov, J. Phys. Chem. B **104**, 3812 (2000).

[10] M. I. Molotskii, R. E. Kris, and V. Fleurov, Phys. Rev. B **51**, 12531 (1995).

[11] R. B. Morgunov, Yu. A. Ossipyan, and Y. Tanimoto, in *Magneto-Science: Magnetic Field Effects on Materials: Fundamentals and Applications*, edited by M. Yamaguchi and Y. Tanimoto (Kodansha, Springer, Tokyo, 2006), p. 281.

[12] A. L. Buchachenko, Zh. Eksp. Teor. Fiz. **132**, 827 (2007) [JETP **105**, 722 (2007)].

[13] A. L. Buchachenko, Pis'ma Zh. Eksp. Teor. Fiz. **84**, 590 (2006) [JETP Lett. **84**, 500 (2006)].

[14] A. L. Buchachenko, Zh. Eksp. Teor. Fiz. **132**, 673 (2007) [JETP **105**, 593 (2007)].

[15] A. L. Buchachenko, Zh. Eksp. Teor. Fiz. **129**, 909 (2006) [JETP **102**, 795 (2006)].

[16] Yu. I. Golovin, R. B. Morgunov, D. V. Lopatin, and A. A. Baskakov, Phys. Status Solidi A **160**, R3 (1997).

[17] Yu. I. Golovin, R. B. Morgunov, and A. A. Dmitrievskii, Mater. Sci. Eng. A **288**, 261 (2000).

[18] L. Dunin-Barkovskii, R. Morgunov, and Y. Tanimoto, Solid State Phenom. **115**, 183 (2006).

[19] Yu. I. Golovin and R. B. Morgunov, Pis'ma Zh. Eksp. Teor. Fiz. **61**, 583 (1995) [JETP Lett. **61**, 596 (1995)].

[20] V. I. Al'shits, N. N. Bekkauer, A. E. Smirnov, and A. A. Urusovskaya, Zh. Eksp. Teor. Fiz. **115**, 951 (1999) [JETP **88**, 523 (1999)].

[21] R. Morgunov, A. Baskakov, I. Blokhin, L. Dunin-Barkovskii, S. Shmurak, and Y. Tanimoto, Solid State Phenom. **115**, 169 (2006).

[22] R. B. Morgunov, S. Z. Shmurak, A. A. Baskakov, B. K. Ponomarev, and V. I. Kulakov, Pis'ma Zh. Eksp. Teor. Fiz. **76**, 366 (2002) [JETP Lett. **76**, 307 (2002)].

[23] Yu. A. Ossipyan, R. B. Morgunov, A. A. Baskakov, S. Z. Shmurak, and Y. Tanimoto, Phys. Status Solidi A **201**, 148 (2004).

[24] J. Rubio O., J. Phys. Chem. Solids **52**, 101 (1991).

[25] A. E. Cordero-Borboa, O. Cano-Corona, A. Clavel-Hernández, and E. Orozco, J. Phys. C: Solid State Physics **19**, 7113 (1986).

[26] J. E. Strutt and E. Lilley, Phys. Status Solidi A **33**, 229 (1976).

[27] N. M. Bannon and J. Corish, Philos. Mag. A **51**, 797 (1985).